Appl. Phys. B 88, 483–492 (2007)
DOI: 10.1007/s00340-007-2719-2

Applied Physics B
Lasers and Optics

A. GROSSEL
V. ZÉNINARI✉
B. PARVITTE
L. JOLY
D. COURTOIS

Optimization of a compact photoacoustic quantum cascade laser spectrometer for atmospheric flux measurements: application to the detection of methane and nitrous oxide

Groupe de Spectrométrie Moléculaire et Atmosphérique, UMR CNRS 6089,
UFR Sciences Exactes et Naturelles, Moulin de la Housse, BP 1039, 51687 Reims Cedex 2, France

Received: 2 March 2007 / Revised version: 21 May 2007
Published online: 11 July 2007 •

ABSTRACT Room temperature (RT) quantum cascade lasers (QCL) are now available even in continuous wave (cw) mode, which is very promising for in situ gas detectors. Ambient air monitoring requires high sensitivity with robust and simple apparatus. For that purpose, a compact photoacoustic setup was combined with two cw QCLs to measure ambient methane and nitrous oxide in the 8 μm range. The first laser had already been used to calibrate the sensitivity of the photoacoustic cell and a detection limit of 3 ppb of CH_4 with a 1s integration time per point was demonstrated. In situ monitoring with this laser was difficult because of liquid nitrogen cooling. The second laser is a new RT cw QCL with lower power, which enabled one to reach a detection limit of 34 ppb of methane in flow. The loss in sensitivity is mainly due to the weaker power as photoacoustic signal is proportional to light power. The calibration for methane detection leads to an estimated detection limit of 14 ppb for N_2O flux measurements. Various ways of modulation have been tested. The possibility to monitor ambient air CH_4 and N_2O at ground level with this PA spectrometer was demonstrated in flux with these QCLs.

PACS 07.88; 92.60.Sz

1 Introduction

Photoacoustic (PA) spectroscopy has proven to be a very sensitive method for gas monitoring. A PA spectrometer is simply composed of a modulated light source and a cell. The detector is a microphone measuring the acoustic wave produced in the cell by the periodic absorption of the modulated light. As any spectroscopic system, a PA detector presents the main advantage of being highly selective. Moreover PA sensors are robust devices that can easily be implemented for in situ monitoring. There is no saturation problems in PA spectroscopy. Thanks to resonant cells and differential measurement techniques, PA sensors have shown excellent sensitivities on the level of ppb for most atmospheric gases. These results are comparable to those of other apparatus, such as multipass cells, but with a generally simpler set-up. Finally PA sensors presents the advantages of a high dynamic range and the possibility to work at atmospheric pressure. One important point in a spectroscopic detection scheme is the light source. Infrared lasers have commonly been used for atmospheric gas measurements in the rovibrational transition range, and QCLs are very suitable for such applications because they emit in the mid-infrared, i.e., the spectral range of fundamental absorption bands of most atmospheric constituents. The PA spectroscopy directly measures the absorption of the molecules and the signal is proportional to the radiation power. Another advantage of using a QCL with PA sensors is, thus, the higher power of these lasers compared with lead salt diode lasers emitting on the same spectral range. A very good sensitivity was demonstrated when combining a PA Helmholtz resonant cell with a continuous wave quantum cascade laser working at liquid nitrogen temperature: a 3 ppb detection limit with a signal to noise ratio of 1 and an 1 s integration time for methane was obtained [1]. Such a sensitivity is more than enough to monitor ambient methane concentration, which lies around 1.8 ppm. Two important spectral ranges can be used for methane measurements: the 3.2–3.3 μm spectral range corresponding to the ν_3 band and the ν_4 band which lies between 7.8 and 8 μm. The second wavelength region is now well accessible with quantum cascade lasers and has been used in several studies [2–6]. Moreover this region is interesting, because it overlaps the ν_1 band of N_2O. It is, therefore, possible to measure both CH_4 and N_2O with a single device.

CH_4 and N_2O are both produced at the Earth's surface and photochemically removed in the stratosphere; they can, thus, serve as markers of large-scale dynamics of the Earth's atmosphere. Measurements performed by satellites or by aircraft campaigns in the stratosphere have been realized to monitor their concentrations versus altitude. The ALIAS spectrometer of the JPL's group for example used lead salt diode lasers to monitor these two gases [7]. More recently a quantum cascade laser was mounted on this spectrometer, enabling one to carry on high altitude measurements. The achieved sensitivity was 2 ppb of methane with a 3 s integration time and an averaging time of two minutes [6]. The precision of measurements was improved by a factor of three thanks to the use of QCLs. Moreover CH_4 and N_2O are active infrared gases and play an important role in global warming. The methane is one of the major greenhouse gases resulting from anthropogenic activities, and it presents a global warming potential 25 times greater

✉ Fax: +33-3-2691-3147, E-mail: virginie.zeninari@univ-reims.fr

than CO_2 [5]. Methane is also involved in complex feedback mechanisms in atmospheric chemistry [2]. Atmospheric methane concentrations have increased from a 700 ppb level 300 years ago to 1.8 ppm nowadays. Emissions originate from both natural sources such as plants oxidation in anaerobic conditions, oceans, wetlands and also human sources: domestic animals, industries, biomass burning, fossil fuel production, etc. Although its sources and sinks are thought to be quite well-known, some processes are yet discussed [8]. The total methane production amount has to be well estimated to establish reliable climate models. That is why sensitive and fast response sensors are needed to measure the strength of the various methane sources. This can be done by fluxes measurements above areas, using eddy-correlation [9, 10]. Agriculture plays a role in methane balance: natural soils are a sink for atmospheric methane, but this oxidation capacity is decreased when the area is transformed into agricultural soils [11]. N_2O emissions are mainly linked to agricultural activities and are influenced by land use; high emissions rates were found above wetland agricultural soils (paddy fields), and above areas after spreading of mineral N fertilizers or animal manure. This phenomenon seems to be a complex and long term effect. N_2O is also a strong greenhouse effect gas: its global warming potential is 310 times that of CO_2, and its concentration has been increasing steadily for one century [5], to reach a level of 310 to 320 ppb at ground level. Its tropospheric concentration is very constant, but its sources repartition is still not well known enough and emissions have to be monitored.

Many techniques have already been proposed to detect methane and nitrous oxide. Spectroscopic techniques have enabled us to reach extremely high sensitivity, which are needed for atmospheric monitoring. The general detection scheme is a mid-infrared source coupled with a multipass cell to enhance absorption and then sensitivity. Lancaster et al. [12] used difference frequency generation to obtain a 3.3 μm radiation. They reached a 0.8 ppb detection limit with a 80 m multipass cell. Real-time measurements were performed with another sensor using different lasers to generate the 3.3 μm radiation and enabled one to quantify ambient methane with a 14 ppb precision [13]. QCLs are very well suited for such measurements as lasers emitting in the 8 μm region have been used for several years. The first one was used by Namjou who performed N_2O and CH_4 sensing with a room-temperature pulsed QCL near 8 μm. He found a noise equivalent absorbance of 5×10^{-5}, and thus a 250 ppb detection limit for N_2O with a 1 m pathlength [3]. Kosterev et al. reached detection limits of 2.5 ppb for methane and 1 ppb for nitrous oxide with a quasi cw QCL and a 100 m multipass cell. The choice of pulsed lasers was made because of the problem of the large heat dissipation in cw lasers, which implied to use liquid nitrogen cooling for such lasers [4]. The recent progresses in QCL technology enable to make cw QCL working at room temperature. Nelson et al. [5] demonstrated a very good sensitivity with a RT pulsed QCL and a 56 m pathlength multipass cell: the detection limit was 4 ppb for methane and 0.7 ppb for nitrous oxide with a 1 s averaging time. Nelson outlines the high sensitivity and response time needed for eddy correlation measurements: precision of 1part per thousand of the ambient mixing ratio is demanded for N_2O, and the working frequency must be at least 10 Hz. Despite their efficiency for gas monitoring, multipass cell sensors present some drawbacks: they are generally quite heavy systems and are very sensitive to optical misalignment. In comparison, PA spectrometers are very simple devices, compact and much less sensitive to the problems of interference fringes and misalignments. They have proved their ability to reach very high sensitivity and methane or nitrous oxide detection in air by a photoacoustic spectrometer has already been demonstrated. For example Kosterev et al. performed a 4 ppb noise equivalent sensitivity in nitrous oxide detection with quartz-enhanced photoacoustic spectroscopy [14]. The application of such devices for atmospheric measurements has been considered by several authors [14, 15]. This article aims to prove the feasibility of ambient air monitoring with a Helmholtz based PA resonator and QCLs.

2 Calibration and optimization of the photoacoustic sensor

2.1 *Experimental setup*

The experimental setup is composed of the laser, a chopper and the cell. The PA cell used for this study has already been presented in [1]. It is an Helmholtz resonator that enables one to realize differential measurements between the two parts of the cell. As the laser beam passes only in one part of the cell, the recorded signal phases are opposite and the difference between them enables one to eliminate most acoustic parasites coming from the outside. This is particularly important because of the low frequency resonance of the cell (315 Hz). Two valves at the middle of the capillaries in the cell enable one to do flow in the cell (see Fig. 1). A mirror was placed just behind the output window of the cell to double the pathlength of the beam. The acoustic signal is recorded by two high sensitivity microphones (Bruel & Kjaer 4179) and sent to a lock-in amplifier to obtain the differential signal between the two parts of the cell. The signals are recorded with a laptop computer via a 16 bits National Instruments data acquisition card.

Until now, the measurements were done in the closed cell, after rest. For real ambient monitoring, a sensor needs

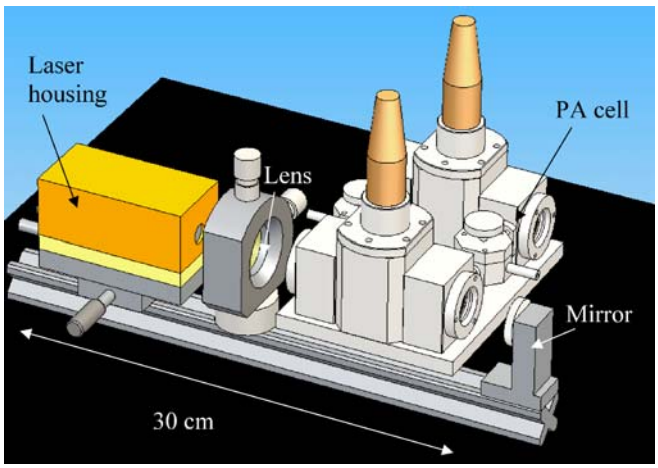

FIGURE 1 Three-dimensional view of the experimental setup: quantum cascade laser mounted in laser housing, lens and PA cell in double pass configuration with a mirror at the end

to be able to work with flow measurements. A new calibration of the sensor was established in flow configuration, to verify that the response remains constant. The presence of flow did not perturb the global response of the PA cell. However a small increase of the noise occurs, generally by a factor two. Consequently the flow was chosen quite slow, with maximum value of 200 mL/min per minute. As the cell volume is weak (approximately 15 cm^3), the time of regeneration of air sample inside is only 4 s in these conditions. This is much weaker than the time required for the air regeneration in multipass cells with a total volume approximately 100 times greater. Calibration of the sensor response was done by flowing in the cell certified mixtures of methane in dry air (Praxair, 103.5 ppm, 21.7 ppm, 10.1 ppm and 2.00 ppm) to verify the proportionality of photoacoustic signal with gas concentration. A flowmeter and a manometer were placed at the input and output of the cell, respectively, for the flow control. All the measurements were done at atmospheric pressure, as it is the general measurement conditions of PA setups.

2.2 *Laser selection*

Two quantum cascade lasers were used for this study. Both are distributed feedback (DFB) and cw commercial lasers, provided by Alpes Lasers. The first one is a liquid nitrogen cooled quantum cascade laser emitting between 1265 and 1273 cm^{-1}. The stronger line of methane on this spectral range is situated at 1270.78 cm^{-1} [16]. The absorption in the region which can be reached with this laser is presented in Fig. 2a. Previous calibration gave a detection limit of 3 ppb on this line with a 1 s integration time and a signal to noise ratio of 1. This laser presents two major drawbacks. Firstly its working temperature requires the use of liquid nitrogen which may causes problems for a portable instrument. Secondly, the spectral range of this QCL coincides with three

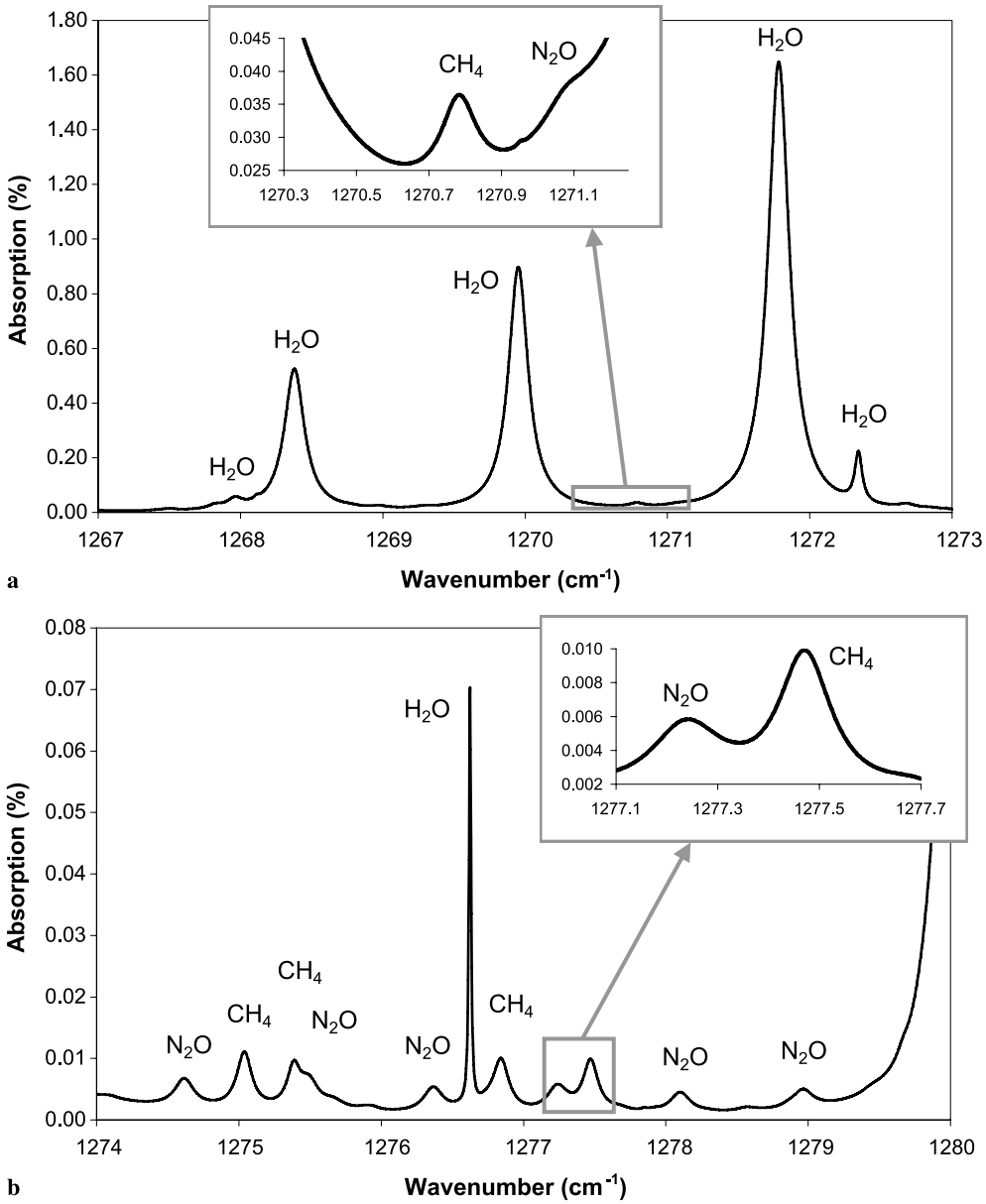

FIGURE 2 Calculated absorption spectra at atmospheric pressure using a Lorentzian line profile on 10 cm for the cryogenic QCL (**a**) and the thermoelectrically cooled QCL (**b**) with 1% of water vapor, 1.8 ppm of methane and 310 ppb of nitrous oxide. Note the difference in y scale between both figures. Water absorption is strong between 1266 and 1272 cm^{-1}

strong water vapor transitions. This is one of the major problems of infrared spectrometers and has to be overcome either by very low pressure or by the careful choice of the laser. As PA measurements cannot be done at too weak pressures because of microphone response loss, the second solution, when possible, is the better one. The choice of the second solution needs a spectral range without water vapor interference and a laser emitting on this region.

The second QCL is a thermoelectrically cooled laser emitting between 1272 and 1283 cm^{-1}. The region reached with this laser is presented in Fig. 2b. Only very weak water lines are present between 1272 and 1279 cm^{-1}. The strongest water line is a doublet at 1276.62 cm^{-1} [16]. Four methane lines can be seen on this wavenumber region, at 1275.04, 1275.38, 1276.84 and 1277.47 cm^{-1}. The last two transitions were used to perform calibration of the sensor and air monitoring because the laser power was higher. According to HITRAN database, the line intensity at 1277.47 cm^{-1} is a little bit weaker than the 1270.78 cm^{-1} one. The laser power is weaker as well: for the methane measurements, the useful power was 8 mW for a working temperature of 283 K instead of 32 mW for the cryogenic laser. Photoacoustic signal is both proportional to the laser power and to the absorption coefficient. This means that in the same experimental conditions with no modifications of the cell response, as expected, a loss of sensitivity of a factor of around six with the RT laser compared to the cryogenic QCL was obtained. This drawback is largely offset by the obtained precision gain thanks to the absence of any strong water line overlapping the methane line. With the cryogenic laser, the water lines hide the N_2O lines, and it was impossible to fit the nitrous oxide concentration. On the contrary, with the room temperature laser, it was possible to quantify methane and nitrous oxide. However sensor calibration was not performed for the nitrous oxide and the response was estimated by using the calibration for methane and the spectroscopic data for N_2O of HITRAN. All the spectroscopic parameters in the two regions are given in Table 1.

2.3 *Photoacoustic sensitivity*

In photoacoustic spectroscopy, the light must be modulated at acoustic frequency to generate a signal in the cell. This can be realized by different ways. The more classical way is amplitude modulation. The beam is periodically interrupted either by a mechanical chopper or, for semiconductor lasers, by a modulation of the injection current between a point below the threshold of the laser and the working current of the laser at the selected wavelength. A scan of wavenumber can then be realized by a slower current ramp or a temperature scan. In that case the photoacoustic signal may be given by [15]:

$$U(\nu, t) = R(\omega)W(\omega, t)N\sigma h(\nu - \nu_0)\,, \tag{1}$$

where U is the microphone signal, $R(\omega)$ is the PA sensor constant, ω is the acoustic pulsation, N the number of absorbing molecules, σ the integral cross section of the line and $h(\nu - \nu_0)$ the line shape, with ν_0 the center line wavenumber. In the case of amplitude modulation, $W(\omega, t)$ corresponds to the mean power in the cell, if we assume that $W(\omega, t) = W_m(1 + e^{i\omega t})$.

Several studies have used wavelength modulation spectroscopy to improve the performance of their sensors. Wavelength modulation is realized by superimposing a small sinusoidal variation of the current onto a slow current scan. This method generates a derivative of the line absorption signal. It is extremely interesting in transmission measurements because it gives an offset free signal. But photoacoustic spectroscopy measures directly absorption and is thus intrinsically a zero background technique. However several authors have tried wavelength modulation with photoacoustic setup and

Laser	Molecule	Vibrational band	Assignment	Wave number (cm^{-1})	Line strength (cm^{-1}/(molecule cm^{-2}))	Air broadening coefficient (cm^{-1}/atm)
Cryo	H_2O	ν_2	$10_{4\,6} \leftarrow 11_{5\,7}$	1267.95310	2.715E-23	0.0619
Cryo	H_2O	ν_2	$7_{2\,6} \leftarrow 8_{3\,5}$	1268.38220	5.527E-22	0.0823
Cryo	CH_4	ν_4	5 F1 3 ← 6 F2 2	1268.97627	3.305E-20	0.0645
Cryo	H_2O	ν_2	$8_{3\,6} \leftarrow 9_{4\,5}$	1269.95724	9.359E-22	0.0794
Cryo	CH_4	ν_4	5 A1 1 ← 6 A2 1	1270.78503	5.604E-20	0.0602
Cryo	N_2O	ν_1	P16	1271.07668	1.552E-19	0.0774
Cryo	H_2O	ν_2	$5_{0\,5} \leftarrow 6_{3\,4}$	1271.78782	1.876E-21	0.0859
Cryo	H_2O	ν_2	$9_{7\,2} \leftarrow 10_{8\,3}$	1272.34362	5.285E-23	0.0287
RT	N_2O	ν_1	P12	1274.61659	1.476E-19	0.0807
RT	CH_4	ν_4	4 F2 3 ← 5 F1 2	1275.04168	3.689E-20	0.0608
RT	CH_4	ν_4	4 E 2 ← 5 E 1	1275.38678	2.457E-20	0.0551
RT	N_2O	ν_1	P11	1275.49294	1.423E-19	0.0817
RT	N_2O	ν_1	P10	1276.36583	1.355E-19	0.0827
RT	H_2O	ν_2	$15_{0\,15} \leftarrow 16_{1\,16}$	1276.62619	5.446E-24	0.0065
RT	H_2O	ν_2	$15_{1\,15} \leftarrow 16_{0\,16}$	1276.62804	1.815E-24	0.0065
RT	CH_4	ν_4	4 F1 3 ← 5 F2 1	1276.84431	3.731E-20	0.0653
RT	N_2O	ν_1	P9	1277.23526	1.270E-19	0.0838
RT	CH_4	ν_4	4 F2 4 ← 5 F1 1	1277.47335	3.739E-20	0.0636
RT	N_2O	ν_1	P8	1278.10121	1.173E-19	0.0849
RT	N_2O	ν_1	P7	1278.96369	1.060E-19	0.0861

TABLE 1 Spectroscopic parameters of molecules that can be detected in the QCLs emitting region. Parameters are from HITRAN database [16]. One can notice the very low value of the broadening coefficient of the unresolved doublet of H_2O at 1276.62 cm^{-1}

concluded that a real gain in signal could be found because of the suppression of the chopper (source of acoustic parasites) and elimination of wall and window noise for powerful beams. In that purpose three different ways of modulation were tested with the RT QCL:

2.3.1 Amplitude modulation. A slow linear current ramp tunes the laser across the target line. Typical amplitude of the ramp was 40 mA to 50 mA, which enables to tune approximately 1 cm^{-1}. The laser beam is mechanically modulated at the resonance frequency of the cell. The integration time was set to 1 s, and scans duration was between 2 and 3 min. A first calibration of the system was realized by this way. Figure 3a. shows a spectrum realized with a slow flow of the certified mixture of 2 ppm of methane.

2.3.2 Wavelength modulation. A sinusoidal modulation of 4 mA amplitude and 315 Hz frequency was added to the current ramp and the first harmonic was recorded. The result is shown on Fig. 3b. with the same mixture flow than Fig. 3a. One can notice that the mean value of Fig. 3b is not exactly 0. This is probably due to the variation of the laser power in the swept range and means that background absorption occurs during experiments.

In practice no improvement was found in recorded spectra between amplitude and wavelength modulation. Typical noise was found to be 0.4 μV with a closed cell, but an increase by a factor of two cannot be avoided when flow is established in the cell. This is probably linked to the very high sensitivity of the microphones used. The results obtained with wavelength modulation seem to prove that the dominant noise in our detector is electronic noise and bad filtering of ambient acoustic level when flowing air in the cell. It must be outlined that the laboratory was not particularly silent as flow was kept by noisy pumps. A more complete study of the noise origin on our set-up has to be performed to improve the measure-

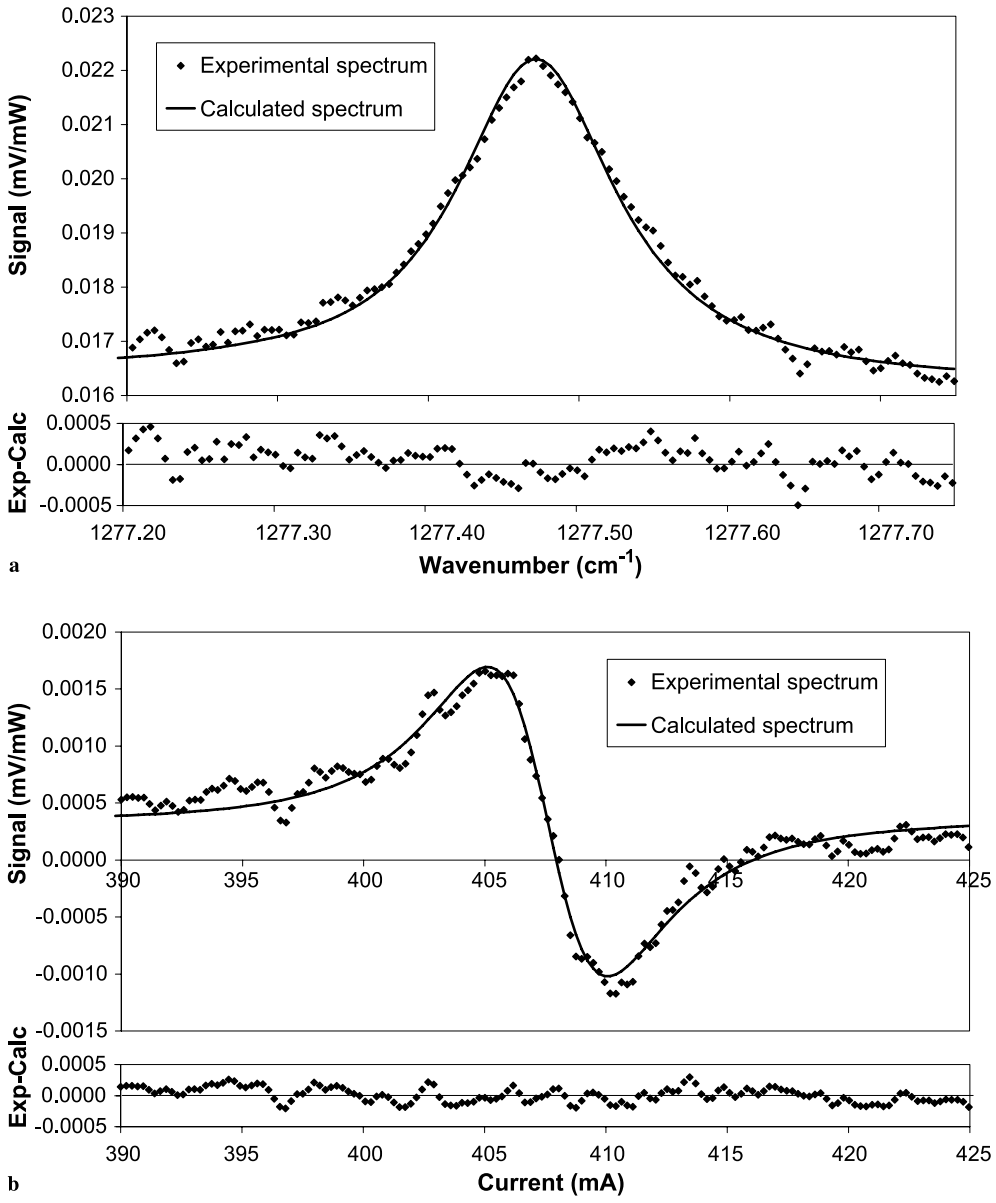

FIGURE 3 (**a**) Photoacoustic signal versus wavenumber. (**b**) Wavelength modulation spectrum obtained in the same experimental conditions versus laser injection current. Both spectra are recorded with flux of certified mixture of 2 ppm of methane in dry air and the RT QCL at 1 s integration per point. The *straight line* represents the fitted spectrum and the *points* correspond to the experimental data. The fit was performed by using HITRAN line parameters, methane concentration and a Lorentzian line profile. The only free parameter was the cell response. The residuals between experimental and fitted spectra are presented in the *lower panels*

ments. Moreover a more complete study has to be done to find the best modulation depth of the sinusoidal modulation. Schilt [17] found that the better results were obtained with a modulation index $m = 2$, where m is defined by:

$$m = \frac{\Delta\upsilon}{\Delta\upsilon_0}, \tag{2}$$

with $\Delta\nu$ the maximum laser frequency deviation and $\Delta\nu_0$ the absorption linewidth. The 4 mA modulation corresponds to an index $m = 0.56$, which means that our measurements were not performed with the maximum response of the detector. Other modulation depths were tested with certified mixtures and showed an increase of the signal until $m = 2$. But it is linked with a widening of the derivative signal. This was a problem for real air measurements because of the presence of several overlapping methane and nitrous oxide lines (see Sect. 3). That is why a lower index m was chosen to enable to fit both CH_4 and N_2O concentrations on the spectra.

2.3.3 On-off modulation. On-off modulation is obtained by a modulation between the top of the line and a point out of the line, generally with a square waveform amplitude modulation of the laser. The obtained signal is directly proportional to the concentration of the target molecules if the line is well isolated. At atmospheric pressure, it is quite impossible to find a wavenumber where no atmospheric molecule absorbs. But the absorption can be low enough to enable very weak error in using this detection method.

In our case, a lock-in detection scheme was used with filtering of the signal at 315 Hz. Signal harmonics above f were, thus, eliminated, and it makes no real difference to use a square or a sinusoidal modulation. This is the reason why a sinusoide at 315 Hz modulates the laser between the top of the line and out of the line. The linearity of the PA sensor response versus methane concentration was verified by this method. Figure 4 shows the signals obtained with different methane concentrations. This method would be very efficient for the realization of an in situ sensor.

2.4 *Obtained detection limits*

General calibration and air measurements were performed by amplitude modulation. Figure 5 shows the calibration with the RT QCL in single and double pass configuration. With the RT QCL, a detection limit of 17 ppb is found for the 1277.47 cm^{-1} methane line in the double pass configuration and of 30 ppb with a single pass in the cell, which was exactly what was expected because of the weaker power and absorption. With this minimum absorption a 12 ppb limit can be estimated for the 1277.23 cm^{-1} N_2O line in single pass configuration, and 7 ppb in double pass configuration. These results are multiplied by two with flux measurements where the noise is two times higher, which leads to a detection limit of 34 ppb of methane and 14 ppb of nitrous oxide. These results are sufficient for the ambient air monitoring of methane and nitrous oxide.

Comparisons between the three methods of modulation were done in single pass configuration. Both wavelength modulation and on-off modulation gave a slightly less good result than the amplitude modulation. With a noise of 0.4 μV, wavelength modulation detection limit was 36 ppb for methane and on-off detection limit was 34 ppb. All these result are very similar.

Photoacoustic detection is an indirect method of measurement. The recorded signal is related to the heat created by the relaxation of excited molecules. At atmospheric pressure, the main way of relaxation is collisions. For the formula (1) to be valid, collisional relaxation time have to be much shorter than the period of laser modulation. This condition is generally well fulfilled in photoacoustic schemes. But a recent study of Schilt [18] has shown that photoacoustic measurements of methane in air can be affected by the resonant vibration to vibration energy transfer occurring in CH_4-O_2 collisions. The relaxation of the vibrationnal state of O_2 is very slow: col-

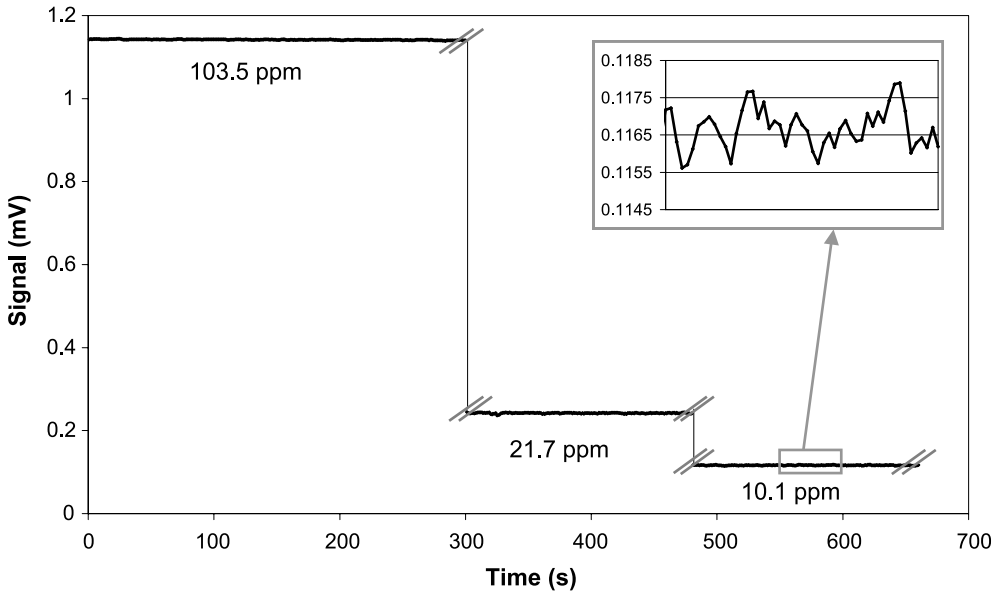

FIGURE 4 Photoacoustic signal versus time when on-off modulation is used with various certified mixtures of methane flown through the cell. The time scale is arbitrary because flux was stopped between each mixture injection

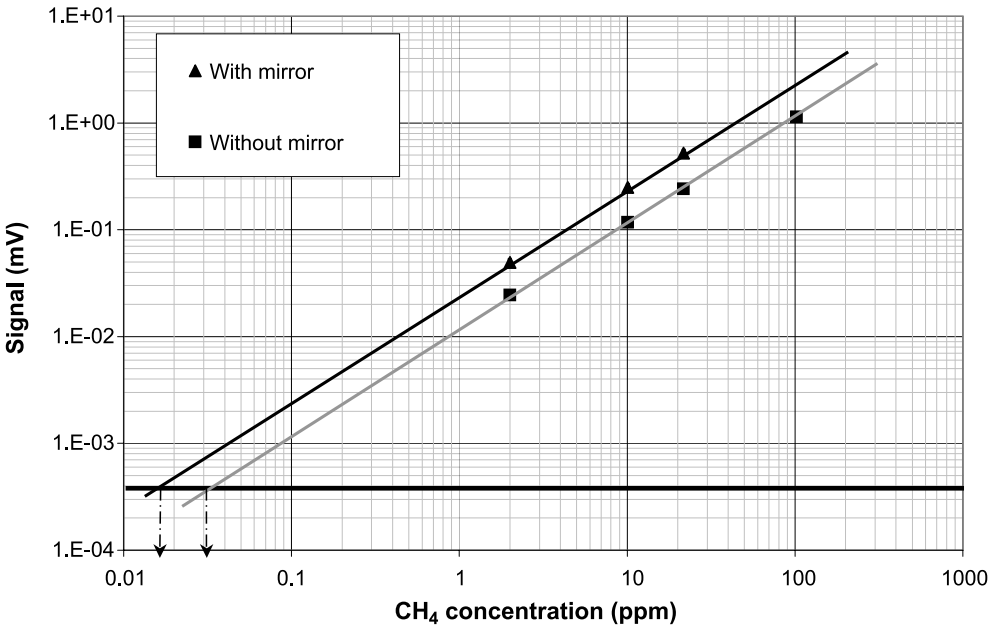

FIGURE 5 Photoacoustic signal versus methane concentration for the line at 1277.47 cm^{-1} This figure shows the calibration results in single pass (without mirror) and double pass configuration (with mirror) for direct absorption and on-off measurements. The signal is clearly proportional to gas concentration as expected in photoacoustic measurements. The detection limit was estimated by extending the straight line until it cuts the noise limit, i.e., at signal to noise ratio of 1. With a noise of 0.4 μV, a detection limit of 30 ppb in single pass and 17 ppb in double pass can be deduced

lisional de-excitation time is 25 ms, which means that it is longer than the acoustic wave period in the cell. Schilt noted then an unexpected parabolic response of his photoacoustic spectrometer versus methane concentration in dry air.

On the other hand, water vapor is known to promote relaxation of O_2 [18, 19]. Calibration with dry air can lead to an under-estimation of the response of the cell. Global response of a photoacoustic spectrometer is expected to increase with humidity in air. We did not notice these issues when calibrating our photoacoustic sensor, even at the weaker methane concentration. This may be explained by a small contamination by water vapor in the cell, even in flow configuration and the weak frequency used (general photoacoustic resonances are in the kHz range). None of our measurements on ambient air leads us to think to a calibration problem due to water vapor because the measurements were done with the cryogenic laser during a very dry period (see next paragraph). Further investigations should be performed to settle whether water vapor amount has an influence on the measurements.

3 Ambient air monitoring

The previous calibration gave the response of the PA sensor for the microphones B&K 4179 (sensitivity 100 mV/Pa) and the 2660 preamplifiers (gain 10×): $R = 715\ \mathrm{V/(W\,cm^{-1})}$. This value was used to quantify methane and nitrous oxide on spectra recorded with air flux in the cell. The signal was divided by the useful light power recorded by a wattmeter placed behind the output window, then it was fitted with a Levenberg Marquardt method to a Lorentzian profile. Lines parameters are fixed to HITRAN values, the only fitted parameter is the molecules target concentration. The water vapor is taken into account on all spectra, thanks to a temperature and humidity probe. Figure 6 shows a spectrum

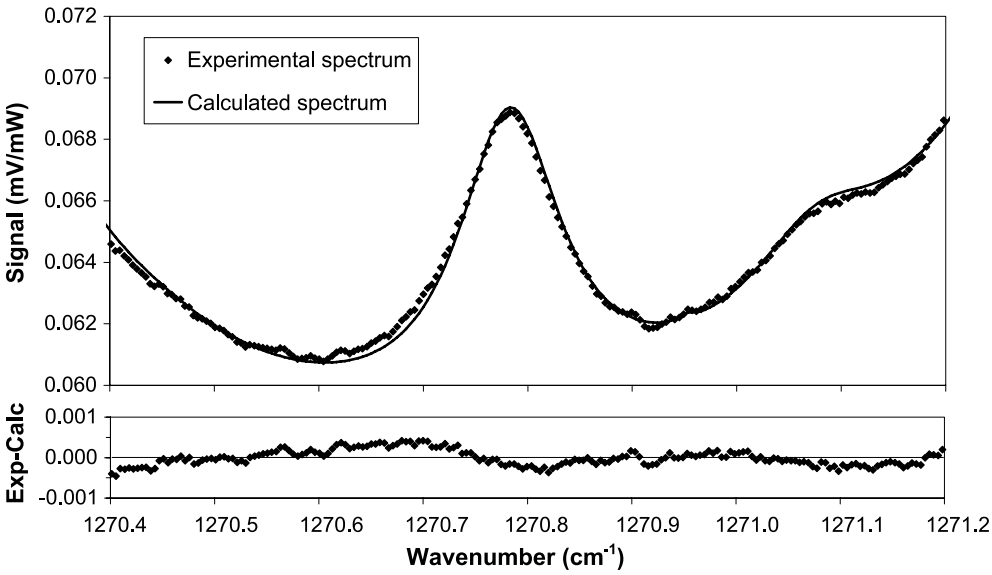

FIGURE 6 Ambient air spectrum obtained with the cryogenic laser. The methane line is situated between two water vapor lines, and a nitrous oxide line can be seen on its right. *Points* are experimental results and the *straight line* is the result of the fit with a Lorentzian profile. The residual between experimental and fitted spectra is presented in the *lower panel*

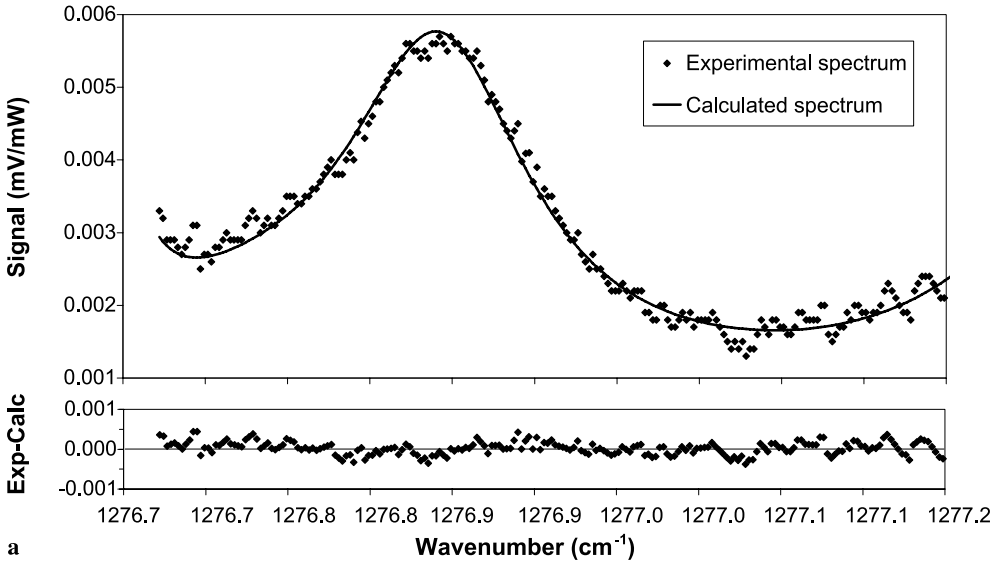

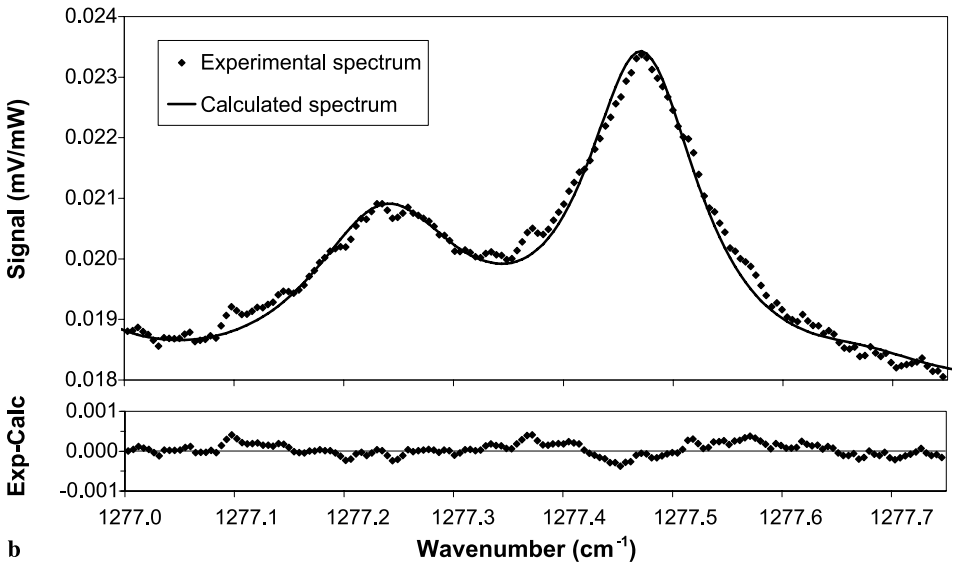

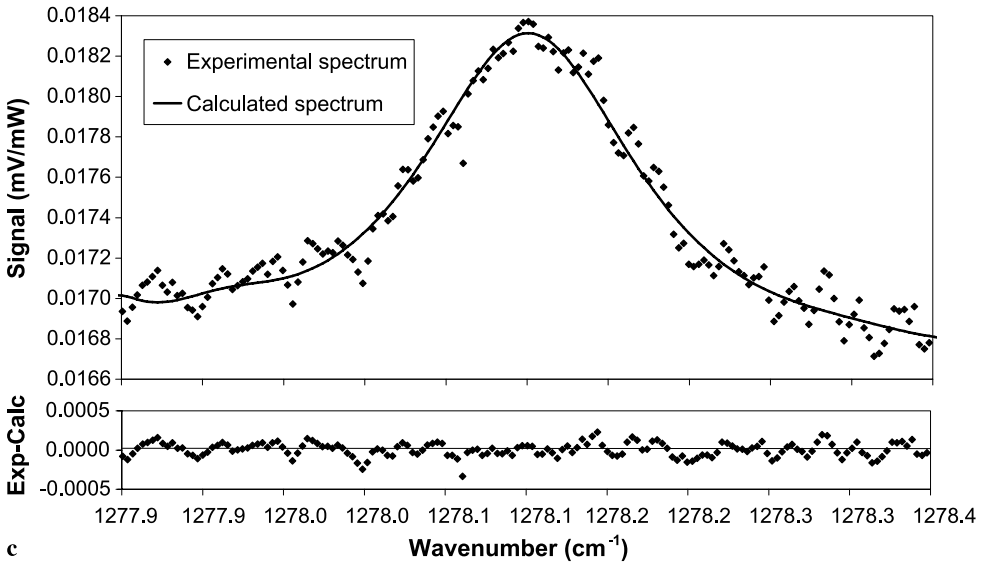

FIGURE 7 Photoacoustic signal versus wavenumber on ambient air recorded with the thermoelectrically cooled laser. The *points* correspond to experimental points and the *straight lines* are the fitted spectra with Lorentzian profile: (**a**) methane line; (**b**) nitrous oxide and methane lines; (**c**) nitrous oxide line

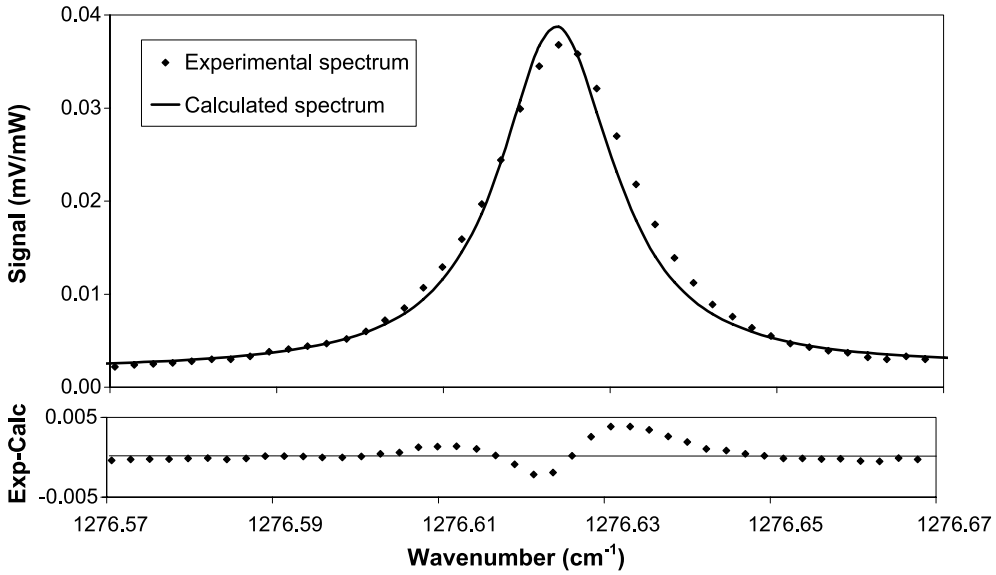

FIGURE 8 Photoacoustic signal versus wavenumber for the water vapor doublet on ambient air. Water vapor was badly fitted on that spectrum which can mean that HITRAN data are not good enough for these lines whose widths are very weak

recorded with the liquid nitrogen cooled QCL. The absorption line corresponds to methane, and the line wings at both sides corresponds to water vapor lines. It was however a rather dry day (only 30% humidity). Water vapor and nitrous oxide concentrations are fixed at the value given by humidity probe and 320 ppb respectively. A nitrous oxide line is visible at 1271 cm^{-1} but the N_2O concentration cannot be fitted with enough precision because of the water vapor line wing. The methane concentration found on this kind of measurements is around 2 ppm, which is quite a high level for ambient air. A possible explanation is that measurements were done with laboratory air and it could have been polluted.

Figure 7 shows results obtained with the thermoelectrically cooled laser. Different working temperatures of the laser enables to scan water vapor, methane and nitrous oxide lines. Figure 7a shows a methane line at 1276.84 cm^{-1}. Figure 7b shows a nitrous oxide line and a methane line. This spectral range was found very useful to fit the concentration of these molecules. Room methane concentration was between 1.9 and 2 ppm and nitrous oxide concentration around 330 ppb, which is a quite high level. Measurements were then made on outside air and the concentrations were found weaker for both gases. Outside methane concentration was generally between 1.82 and 1.89 ppm and nitrous oxide concentration between 307 and 335 ppb. The spectrum on Fig. 7c shows an isolated N_2O line, which can also be used for the N_2O concentration measurements.

Finally Fig. 8 shows a fit of the water vapor doublet at 1276.62 cm^{-1}. This figure demonstrates the possibility to also obtain the water vapor concentration. However water vapor was badly fitted on that spectrum which can mean that HITRAN data are not good enough for these lines whose widths are very weak.

4 Conclusion

The possibility of ambient methane and nitrous oxide flux measurements with a compact PA Helmholtz resonant cell and QCLs was demonstrated. Our results lead to very good detection limits in flux measurements: 34 ppb of methane and 14 ppb of nitrous oxide in air at atmospheric pressure. Water vapor could also be measured but it would need a complete spectroscopic study of the parameters of the water doublet at 1276.62 cm^{-1}. Our system can be used to make sensitive and simple in situ sensors. The best practical modulation way is on-off modulation where the obtained signal is directly related to the molecular concentration. The detection limits obtained are of the same order of magnitude than that of typical multipath absorption spectroscopy systems. The main advantages of photoacoustic spectrometers in comparison to these systems are the compactness of the system, the ease of use, the working at atmospheric pressure, the insensitivity to optical misalignment and the very weak volume of the cell giving the possibility to install the sensor in a moving system and, as the cell volume is very low, to make real-time in situ measurements at quite a high speed.

ACKNOWLEDGEMENTS The authors want to acknowledge Vincent Parpillon and Thomas Decarpenterie for their technical help. Agnès Grossel also wants to acknowledge the financial support of the Délégation Générale à l'Armement.

REFERENCES

1 A. Grossel, V. Zeninari, L. Joly, B. Parvitte, D. Courtois, G. Durry, Spectrochim. Acta A **63**, 1021 (2006)
2 A.A. Kosterev, R.F. Curl, F.K. Tittel, C. Gmachl, F. Capasso, D.L. Sivco, J.N. Baillargeon, A.L. Hutchinson, A.Y. Cho, Opt. Lett. **24**, 1762 (1999)
3 K. Namjou, S. Cai, E.A. Whittaker, J. Faist, C. Gmachl, F. Capasso, D.L. Sivco, A.Y. Cho, Opt. Lett. **23**, 219 (1998)
4 A.A. Kosterev, R.F. Curl, F.K. Tittel, C. Gmachl, F. Capasso, D.L. Sivco, J.N. Baillargeon, A.L. Hutchinson, A.Y. Cho, Appl. Opt. **39**, 4425 (2000)
5 D.N. Nelson, B. McManus, S. Urbanski, S. Herndon, M.S. Zahniser, Spectrochim. Acta A **60**, 3325 (2004)
6 C.R. Webster, G.J. Flesch, D.C. Scott, J.E. Swanson, R.D. May, W.S. Woodward, C. Gmachl, F. Capasso, D.L. Sivco, J.N. Baillargeon, A.L. Hutchinson, A.Y. Cho, Appl. Opt. **40**, 321 (2001)
7 C.R. Webster, R.D. May, C.A. Timble, R.G. Chave, J. Kendall, Appl. Opt. **33**, 454 (1994)
8 F. Keppler, J.G. Hamilton, M. Brass, T. Rockmann, Nature **439**, 187 (2006)
9 P. Werle, R. Kormann, Appl. Opt. **40**, 846 (2001)
10 R. Kormann, H. Muller, P. Werle, Atmosph. Environ. **35**, 2533 (2001)
11 P. Boeckx, O. Van Cleemput, Nutrient Cycl. Agroecosyst. **60**, 35 (2001)

12 D.G. Lancaster, D. Richter, R.F. Curl, F.K. Tittel, L. Goldberg, J. Koplow, Opt. Lett. **24**, 1744 (1999)
13 D.G. Lancaster, R. Weidner, D. Richter, F.K. Tittel, J. Limpert, Opt. Commun. **175**, 461 (2000)
14 A.A. Kosterev, Y.A. Bakhirkin, F.K. Tittel, Appl. Phys. B **80**, 133 (2005)
15 M. Szakall, H. Huszar, Z. Bozoki, G. Szabo, Infrared Phys. Technol. **48**, 192 (2006)
16 L.S. Rothman, D. Jacquemart, A. Barbe, D. Chris Benner, M. Birk, L.R. Brown, M.R. Carleer, C. Chackerian Jr., K. Chance, L.H. Coudert, V. Dana, V.M. Devi, J.-M. Flaud, R.R. Gamache, A. Goldman, J.-M. Hartmann, K.W. Jucks, A.G. Maki, J.-Y. Mandin, S.T. Massie, J. Orphal, A. Perrin, C.P. Rinsland, M.A.H. Smith, J. Tennyson, R.N. Tolchenov, R.A. Toth, J. Vander Auwera, P. Varanasi, G. Wagner, J. Quantum Spectrosc. Radiat. Transf. **96**, 139 (2005)
17 S. Schilt, L. Thévenaz, Infrared Phys. Technol. **48**, 154 (2006)
18 S. Schilt, J.P. Besson, L. Thévenaz, Appl. Phys. B **82**, 319 (2006)
19 F.G.C. Bijnen, F.J.M. Harren, J.H.P. Hackstein, J. Reuss, Appl. Opt. **35**, 5357 (1996)